Int J Adv Manuf Technol (2007) 32: 229–237
DOI 10.1007/s00170-005-0332-2

ORIGINAL ARTICLE

Jih-Hua Chin · Shou-Der Sheu

Strengths and weaknesses of finite element modeling deep hole drilling as compared with beam and column equations

Received: 22 March 2004 / Accepted: 5 September 2005 / Published online: 21 March 2006

Abstract Deep hole drilling has been studied mainly experimentally in the past. Recently, some theories using beam or column equations have been proposed, which involved complicated mathematical efforts. This work analyzed deep hole drilling by a finite element model (FEM). Results of modal analysis on the established FEM were compared with results from Euler beam equations. Further analysis showed that the FEM could also predict straightness deviation as did the column equation. In addition, FEM could analyze the effects of variable support distance which neither beam nor column equation could. Other analysis results are also presented. The results in this study showed the strength and weakness of the FEM.

Keywords Deep hole drilling · Finite element model · Column · Beam theory · Hole straightness

1 Introduction

Deep-hole drilling is a high quality manufacturing process extensively used in the defense, automotive and aviation industries. It produces holes of high accuracy in terms of size, parallelism, straightness and surface finish. There are three types of deep-hole drilling: gun drilling, BTA (boring and trepanning association) drilling and ejector drilling.

J.-H. Chin (✉) · S.-D. Sheu
Department of Mechanical Engineering,
National Chiao Tung University,
1001 Tashue Road,
Hsinchu, Taiwan, 300, Republic of China
e-mail: jhchin@mail.nctu.edu.tw
Tel.: +886-3-5731965
Fax: +886-3-5727485

Early research on deep hole drilling focused mainly on the hole qualities with respect to drilling conditions [1–3], or specific phenomenon like chip congestion [4, 5]. Later studies established the force system [6, 7].

Since the tool shaft in deep hole drilling is extraordinarily long, an early study revealed that the influence of its dynamics on the drilling process may not be neglected [8]. A series of studies on the tool shaft were conducted by Chin and Lee [9], Chin et al. [10], Perng and Chin [11], and Deng et al. [12].

The equations for tool shaft are mathematically complicated and require the column equation [12] to predict straightness and the beam equation [9, 10] to describe tool lateral motion. The purpose of this study is to investigate the strength and weakness of a finite element model which replaces both column and beam equations at the same time.

A finite element model was used by Kakade and Chow [13] in studying boring distortion; but boring is different from BTA drilling. The BTA drilling has a longer shaft and no temperature effects because of the cutting fluid. A different model is established and investigated in this study.

2 Finite element of BTA system

The BTA machining analysis system can be characterized by two coordinate systems: the fixed coordinates (X-Y-Z), and the rotating coordinates (x-y-z), as shown in Fig. 1.

2.1 Finite element coordinates and shape function

Each sub-element of the tool shaft of BTA drilling is considered to be initially straight and is modeled as an eight degree of freedom element: two translations (u,v) and two rotations (θu,θv) at each end-point of the element (Fig. 2).

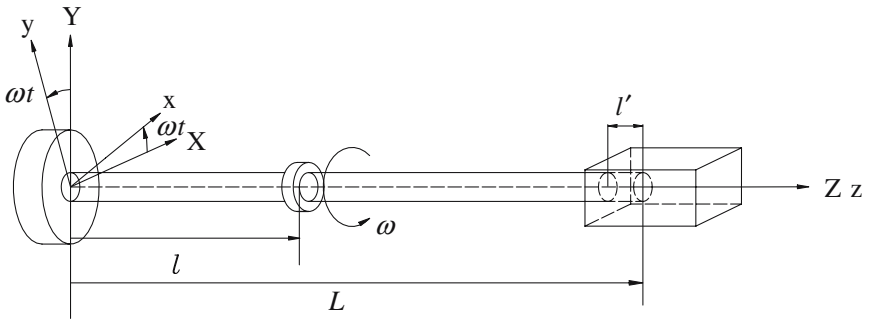

Fig. 1 Coordinate systems of BTA machining

2.2 Element and system equation

The element equations of a spinning drill shaft can be determined by using Hamilton's principle [14]:

$$I = \int_{t1}^{t2} (T - V + W)dt \tag{1}$$

where T and V are the kinetic and potential energies and W is the virtual work done by the drilling forces of the element.

The total kinetic energy is

$$T^e = \frac{1}{2}m\int_0^{l_e}\begin{Bmatrix}\dot{u}\\ \dot{v}\end{Bmatrix}^T\begin{Bmatrix}\dot{u}\\ \dot{v}\end{Bmatrix}ds + \frac{1}{2}\int_0^{l_e} I_d^e\begin{Bmatrix}\dot{\theta}u\\ \dot{\theta}v\end{Bmatrix}^T\begin{Bmatrix}\dot{\theta}u\\ \dot{\theta}v\end{Bmatrix}ds + \frac{1}{2}\int_0^{l_e} I_p^e\dot{\phi}^2 ds - \dot{\phi}\int_0^{l_e} I_p^e\dot{\theta}u\dot{\theta}v ds \tag{2}$$

The total potential energy is

$$V^e = \frac{1}{2}\int_0^{l_e} EI\begin{Bmatrix}u''\\ v''\end{Bmatrix}^T\begin{Bmatrix}u''\\ v''\end{Bmatrix}ds + \frac{1}{2}\int_0^{l_e} F_w\begin{Bmatrix}u'\\ v'\end{Bmatrix}^T\begin{Bmatrix}u'\\ v'\end{Bmatrix}ds \tag{3}$$

The virtual work is

$$\delta W^e = \int_0^{l_e}\begin{Bmatrix}\delta u\\ \delta v\end{Bmatrix}^T\begin{Bmatrix}F_u\\ F_v\end{Bmatrix}ds \tag{4}$$

The finite element motion equation of the BTA spinning shaft can be obtained from Eqs. 1, 2, 3, 4:

$$\mathbf{M}_e\ddot{\mathbf{q}}_e + \mathbf{C}_e\dot{\mathbf{q}}_e + \mathbf{K}_e\mathbf{q}_e = \mathbf{F}_e \tag{5}$$

From Eq. 5, the motion equation can be represented in the rotating coordinate system as follows:

$$\mathbf{M}_e'\ddot{\mathbf{p}}_e + \mathbf{C}_e'\dot{\mathbf{p}}_e + \mathbf{K}_e'\mathbf{p}_e = \mathbf{F}_e'$$

The assembled system equation of motion is obtained by superposition of each sub-element as follows:

$$\mathbf{M}\ddot{\mathbf{D}} + \mathbf{C}\dot{\mathbf{D}} + \mathbf{K}\mathbf{D} = \mathbf{F} \tag{6}$$

where $\mathbf{M}$ is the symmetric mass matrix, $\mathbf{C}$ is the skew symmetric matrix which is dependent on the rotational speed, $\mathbf{K}$ is usually the symmetric stiffness matrix and $\mathbf{F}$ is the loading force vector.

2.3 The elements from ANSYS

Several types of structural analysis are available in the ANSYS [15] family of products: Static, Modal, Harmonic, Transient Dynamic and Spectrum Analysis. The PIPE16 element was selected to build the tool shaft of Fig. 1. Every element length is 25 mm. PIPE16 is a uniaxial element with tension-compression, torsion, and bending capabilities. The three-dimensional beam element has six degrees of freedom at two nodes: translations in the nodal x, y and z directions and rotations about the nodal x-, y- and z-axes.

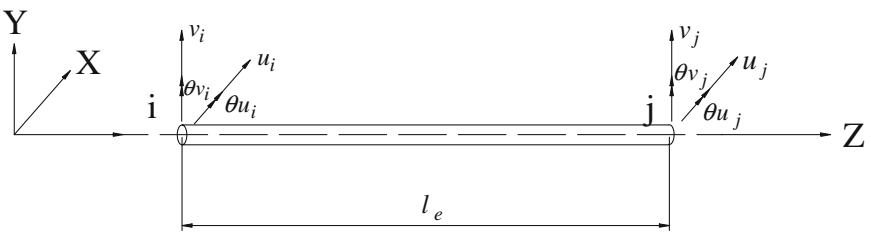

Fig. 2 Typical finite shaft element of BTA

3 Analysis using ANSYS model

3.1 Modal analysis on ANSYS model

The purpose of this analysis is to evaluate the ANSYS model and compare it with the beam equation [9] by modal analysis. The tool data are: tool head diameter=18.91(mm), drill tube length=1,600(mm), internal diameter of drill tube=11.5(mm) and external diameter of drill tube=17(mm).

Type 1. System eigenproperties—solid shaft

The equation of motion without fluid in the lateral direction is as follows [9]:

$$EI_s \frac{\partial^4 X}{\partial s^4} + \rho_s A_s \frac{\partial^2 X}{\partial t^2} + C \frac{\partial X}{\partial t} - \rho_s I_s \frac{\partial^4 X}{\partial s^2 \partial t^2} = 0 \tag{7}$$

The equation can be simplified to become an Euler beam equation:

$$EI_s \frac{\partial^4 X}{\partial s^4} + \rho_s A_s \frac{\partial^2 X}{\partial t^2} + C \frac{\partial X}{\partial t} = 0 \tag{8}$$

Type 2. System eigenproperties—solid shaft with static fluid

The equation of motion with static fluid in the lateral direction is as follows [9]:

$$EI_s \frac{\partial^4 X}{\partial s^4} + \left(\rho_s A_s + \rho_f A_f\right) \frac{\partial^2 X}{\partial t^2} + C \frac{\partial X}{\partial t} - \left(\rho_s I_s + \rho_f I_f\right) \frac{\partial^4 X}{\partial s^2 \partial t^2} = 0 \tag{9}$$

Table 1 Natural frequencies of lateral vibration of the shaft of a BTA drill (hanged horizontally without fluid)

Mode	Analysis values of ANSYS (Hz)	Theoretical values of Euler beam (Hz)	Theoretical values of equation [9] (Hz)	Experimental values [9] (Hz)
1	36.521	36.538	36.522	38.572
2	100.60	100.718	100.629	103.469
3	196.95	197.447	197.170	199.699
4	325.90	326.390	325.541	326.396
5	485.60	487.571	482.673	492.157
6	678.24	680.987	677.275	693.670
7	918.09	906.640	900.084	914.559
8	1,167.3	1,164.528	1,153.745	1,178.076

Table 2 Natural frequencies of lateral vibration of the shaft of a BTA drill (hanged horizontally with static fluid)

Mode	Analysis values of ANSYS (Hz)	Theoretical values of Euler beam (Hz)	Theoretical values of equation [9] (Hz)	Experimental values [9] (Hz)
1	34.933	34.989	34.935	34.877
2	96.235	96.338	96.258	96.881
3	188.66	188.861	188.612	189.887
4	311.73	312.195	311.432	313.895
5	464.49	466.368	464.658	472.781
6	648.75	651.373	648.028	654.917
7	878.18	867.213	861.305	868.056
8	1,116.5	1,113.887	1,104.167	1,116.072

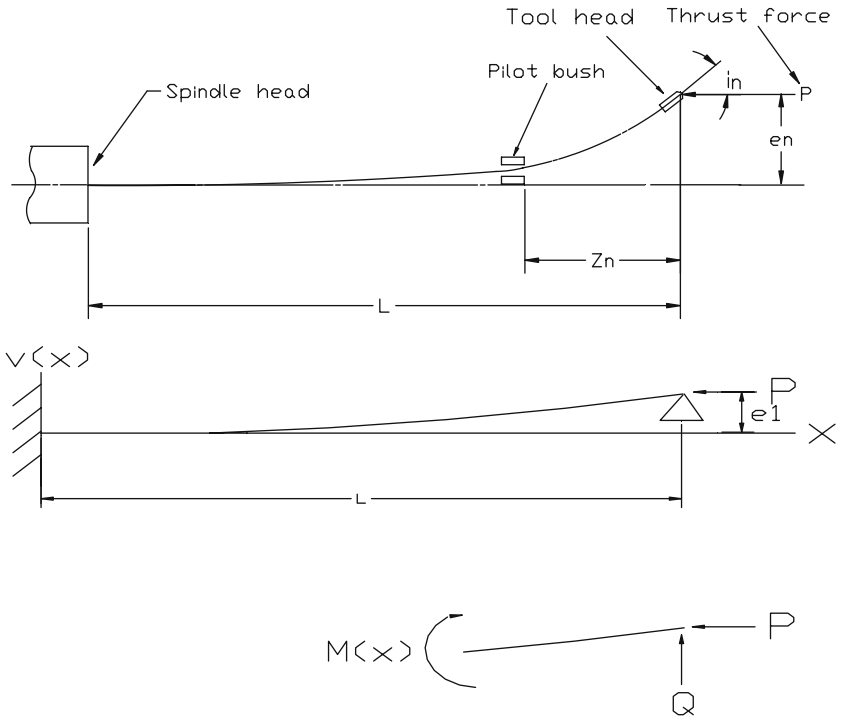

Fig. 3 Moment diagram of tool shaft pilot bush misalignment

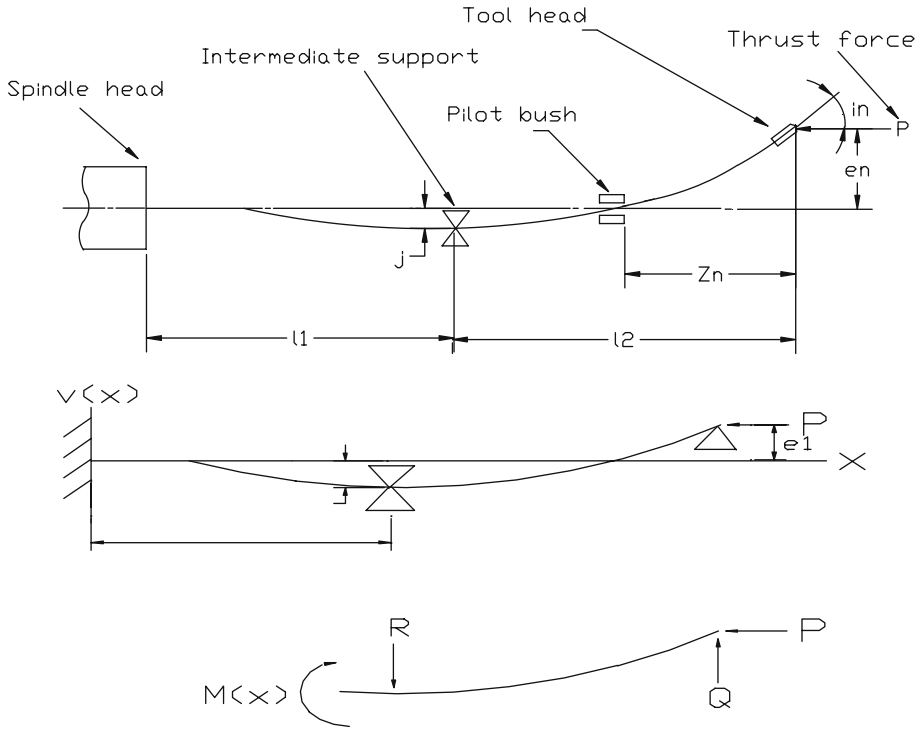

Fig. 4 Moment diagram of pilot bush and support misalignment of tool shaft

The equation can be simplified to become an Euler beam equation:

$$EI_s \frac{\partial^4 X}{\partial s^4} + \left(\rho_s A_s + \rho_f A_f\right) \frac{\partial^2 X}{\partial t^2} + C \frac{\partial X}{\partial t} = 0 \tag{10}$$

The following boundary conditions are valid for Types 1 and 2:

$$\begin{aligned} s = 0, \frac{\partial^2 X}{\partial s^2} = \frac{\partial^3 X}{\partial s^3} = 0 \\ s = l, \frac{\partial^2 X}{\partial s^2} = \frac{\partial^3 X}{\partial s^3} = 0 \end{aligned} \tag{11}$$

Natural frequency comparisons of lateral vibration generated from different models are listed in Tables 1 and 2.

3.2 Straightness analysis by ANSYS model

Sakuma et al. [16] proposed a simple equation to describe the hole straightness deviation due to pilot bushing misalignment:

$$e_n = \left(1 + \frac{3\Delta Z}{2L}\right)^n \delta_B \tag{12}$$

This equation excluded the effects of thrust force and bending; it also excluded parameters such as tool diameter and Young's modulus of the shaft. Deng et al. [12] proposed an equation to consider all these effects:

$$e_n = \left[1 + \frac{\lambda(1 - \cos \lambda L)}{\sin \lambda L - L\lambda \cos \lambda L} \Delta X\right]^n \delta_B \tag{13}$$

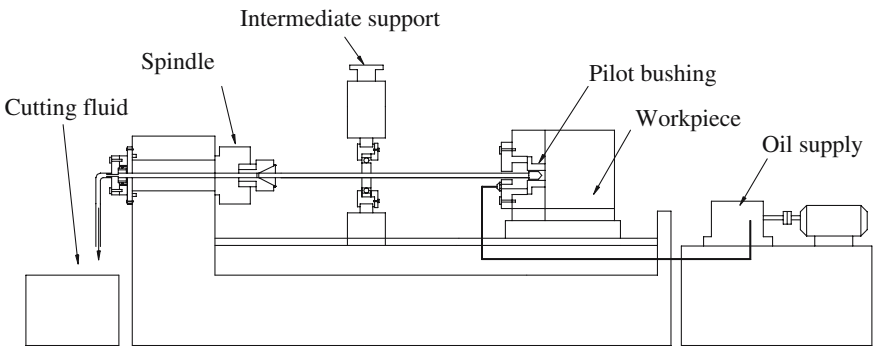

Fig. 5 BTA machining system

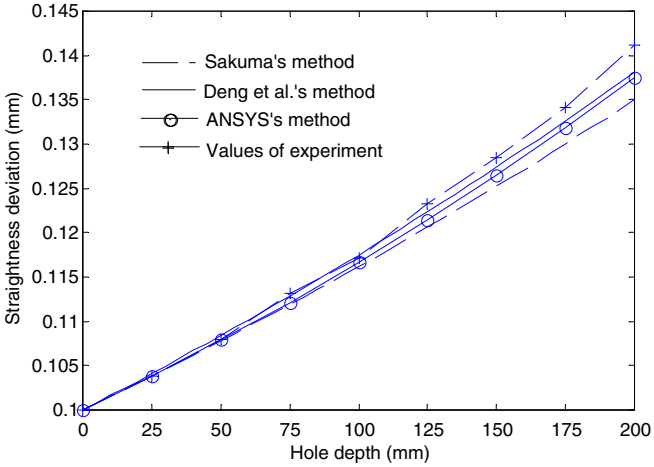

Fig. 6 Axial hole straightness deviation. Pilot bush misalignment=0.1 mm; tool length=1,000 mm

$$where\ \ \lambda = \sqrt{\frac{P}{EI}}$$

The ANSYS model is able to predict the straightness deviation caused by pilot bushing and support misalignments which were studied by Sakuma et al. [16] and Deng et al. [12].

Case 1: The effect of pilot bushing misalignments (Fig. 3)

The drill shaft deflection was described by Deng et al. [12] as

$$EI\frac{d^2y}{dx^2} = P(\delta_B - y) + Q(L - x)$$

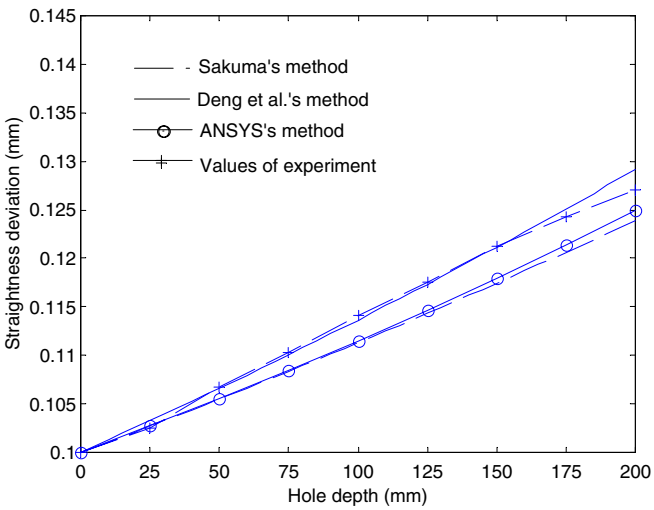

Fig. 7 Axial hole straightness deviation. Pilot bush misalignment=0.1 mm; tool length=1,400 mm

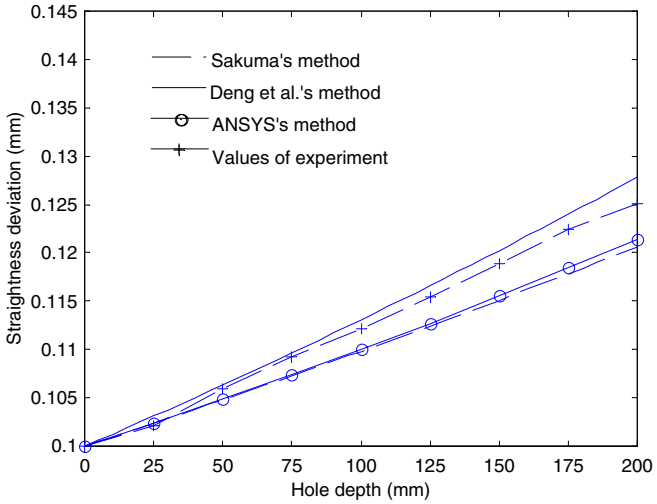

Fig. 8 Axial hole straightness deviation. Pilot bush misalignment=0.1 mm; tool length=1,600 mm

with boundary conditions:

$$y(0) = 0 \quad y'(0) = 0 \quad y(L) = \delta_B$$

Case 2: The effect of support misalignments (Fig. 4)

The drill shaft deflection was described by Deng et al. [12] as

$$EI\frac{d^2y_1}{dx^2} = P(\delta_B - y) + Q(L - x) - R(\ell_1 - x) \quad 0 \le x \le \ell_1$$

$$EI\frac{d^2y_2}{dx^2} = P(\delta_B - y) + Q(L - x) \quad \ell_1 \le x \le L$$

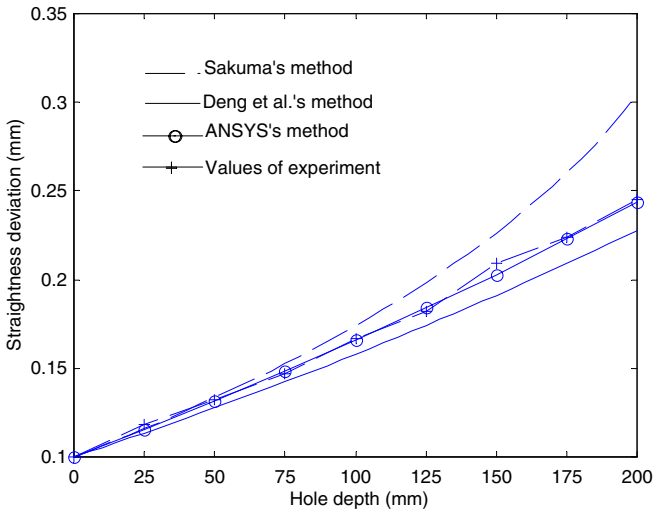

Fig. 9 Axial hole straightness deviation. Pilot bush misalignment=0.1 mm; tool length=1,000 mm; intermediate support misalignment=0.1 mm; intermediate support location=$L/4$

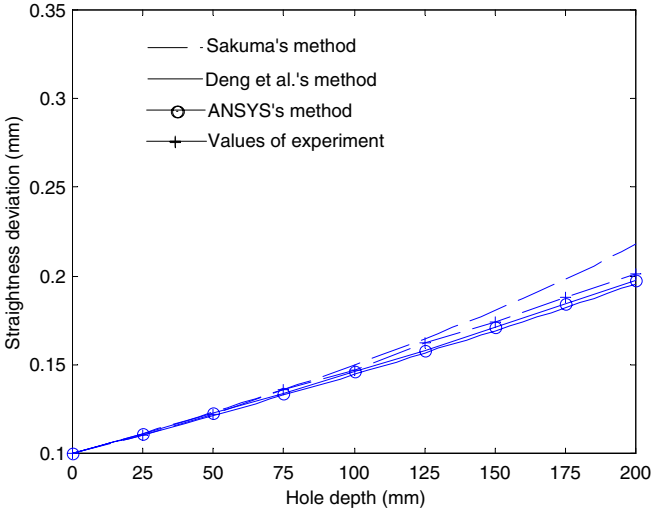

Fig. 10 Axial hole straightness deviation. Pilot bush misalignment=0.1 mm; tool length=1,400 mm; intermediate support misalignment=0.1 mm; intermediate support location=$L/4$

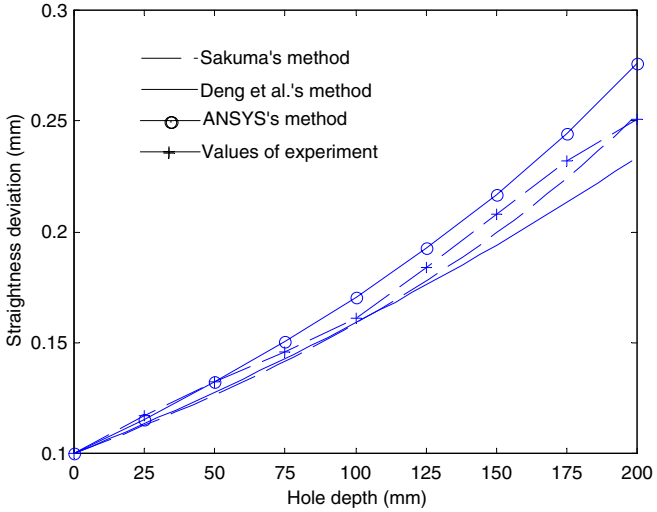

Fig. 12 Axial hole straightness deviation. Pilot bush misalignment=0.1 mm; tool length=1,000 mm; intermediate support misalignment=0.1 mm; intermediate support location=$L/2$

With boundary conditions:

$$y_1(0) = 0 \quad y_1(l_1) = y_2(l_1) = -\delta_s \quad y_2(L) = \delta_B$$
$$y_1'(0) = 0 \quad y_1'(l_1) = y_2'(l_1)$$

3.3 Experiments for comparison of straightness deviation

In order to offer a comparison basis, experiments on a retrofitted deep hole drilling machine (Fig. 5) were conducted. Material of the workpiece was AISI_C1020. The tool head diameter was 18.91 mm.

If the bush misalignment exists, the misalignment builds an initial inclination [12]. A longer shaft alleviates that angle, hence producing a smaller straightness deviation. The comparison of results is shown in Figs. 6, 7, 8.

The location of the intermediate support also influences the straightness. Support location is the distance l in Fig. 1. Figures 9, 10, 11 show the comparative results for support location $l = L/4$. Figures 12, 13, 14 show the results for support location $l = L/2$ and Figs. 15, 16, 17 for $l = 3L/4$.

Direct comparisons between the ANSYS model and experiments with respect to effect of different shaft lengths on the straightness are seen in Figs. 18, 19, 20.

3.4 Analysis of the influence of variable support distance

The FEM model is able to analyze the influence of variable intermediate support location. In Fig. 1, if the distance

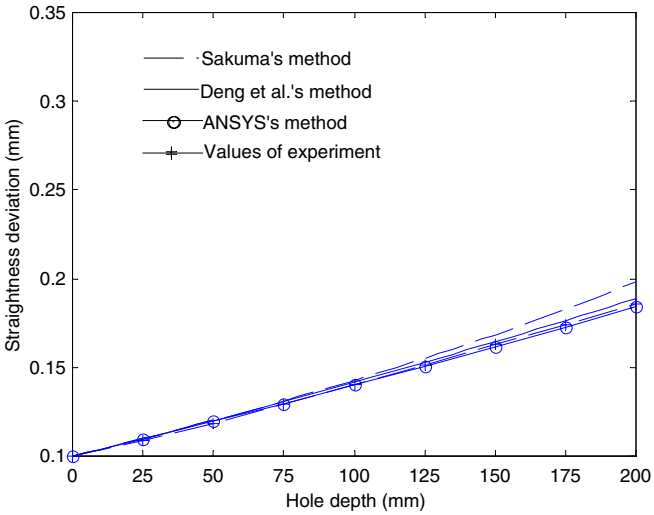

Fig. 11 Axial hole straightness deviation. Pilot bush misalignment=0.1 mm; tool length=1,600 mm; intermediate support misalignment=0.1 mm; intermediate support location=$L/4$

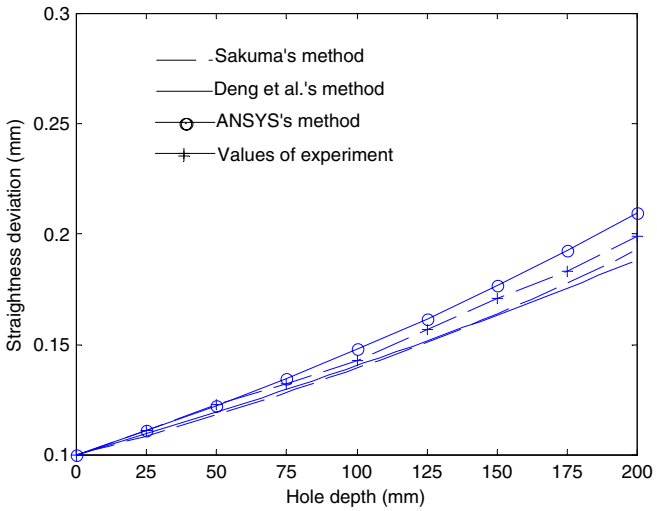

Fig. 13 Axial hole straightness deviation. Pilot bush misalignment=0.1 mm; tool length=1,400 mm; intermediate support misalignment=0.1 mm; intermediate support location=$L/2$

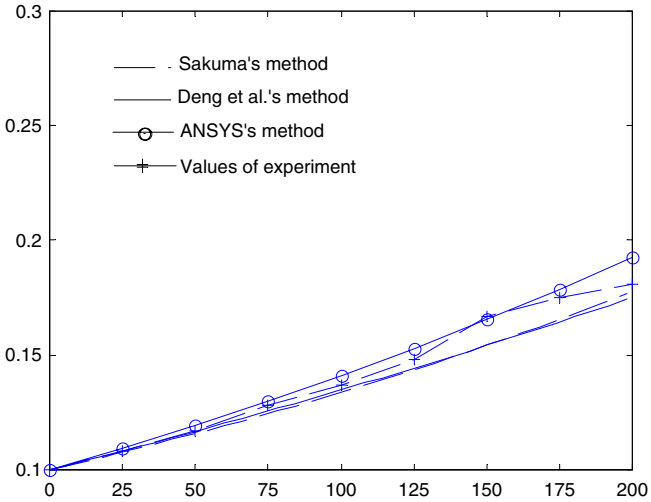

Fig. 14 Axial hole straightness deviation. Pilot bush misalignment=0.1 mm; tool length=1,600 mm; intermediate support misalignment=0.1 mm; intermediate support location=$L/2$

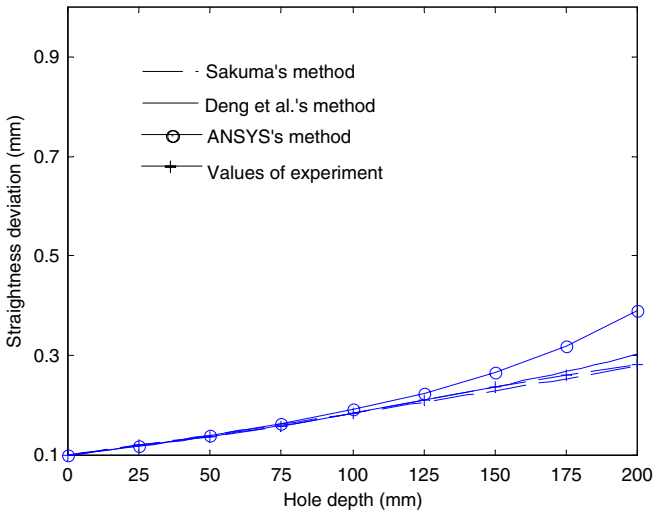

Fig. 16 Axial hole straightness deviation. Pilot bush misalignment=0.1 mm; tool length=1,400 mm; intermediate support misalignment=0.1 mm; intermediate support location=$3L/4$

between the support and the bushing is L_{ps} then the following relation holds:

$$L = l + l' + L_{ps} \tag{14}$$

In the retrofitted machine (Fig. 6), the workpiece was carried by the carriage while the tool rotated. Hence, constant l means fixed support distance and constant L_{ps} means variable support distance as shown in Figs. 21 and 22.

4 Discussions

Modal analysis of the ANSYS model enables a comparison of natural frequency with beam equations. Tables 1 and 2 list the natural frequencies of the first eight modes produced by different mechanisms. It is seen that the errors between different mechanisms are negligibly small. The validity of the FEM built is thus proven. Since the beam equation is mathematically involved, the FEM becomes a very convenient alternative.

Deng et al. [12] showed that for fixed bush misalignment longer tool shaft produces smaller straightness deviations. Figures 6, 7, 8, 9 compare the effect of shaft length from different mechanisms. It is seen that Deng et al.'s model is the closest to experimental results while the FEM model is roughly close to Sakuma et al.'s model. The trend is more apparent for longer shafts as shown in Figs. 8 and 9. Since Sakuma et al.'s model is a rather primitive one, the comparison reveals that FEM is less accurate in predicting the straightness deviation induced by bush misalignment.

Some very interesting results can be seen from Figs. 9, 10, 11, 12, 13, 14, 15, 16, 17, 18, 19, 20 in which both bush

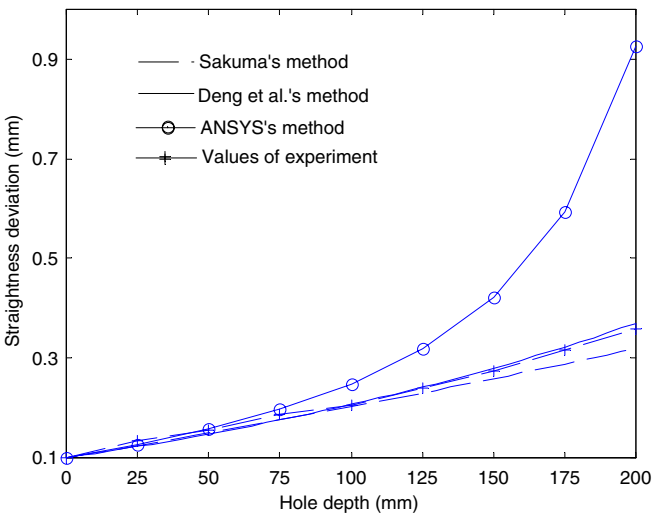

Fig. 15 Axial hole straightness deviation. Pilot bush misalignment=0.1 mm; tool length=1,000 mm; intermediate support misalignment=0.1 mm; intermediate support location=$3L/4$

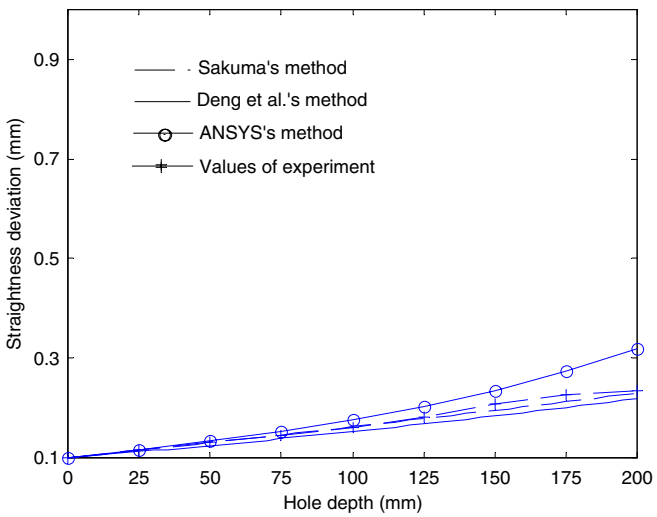

Fig. 17 Axial hole straightness deviation. Pilot bush misalignment=0.1 mm; tool length=1,600 mm; intermediate support misalignment=0.1 mm; intermediate support location=$3L/4$

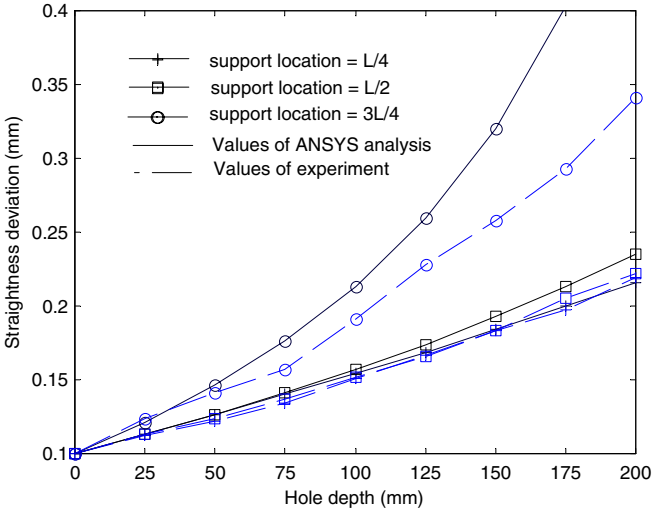

Fig. 18 Hole straightness deviation. Pilot bush misalignment=0.1 mm; tool length=1,200 mm; intermediate support misalignment=0.1 mm

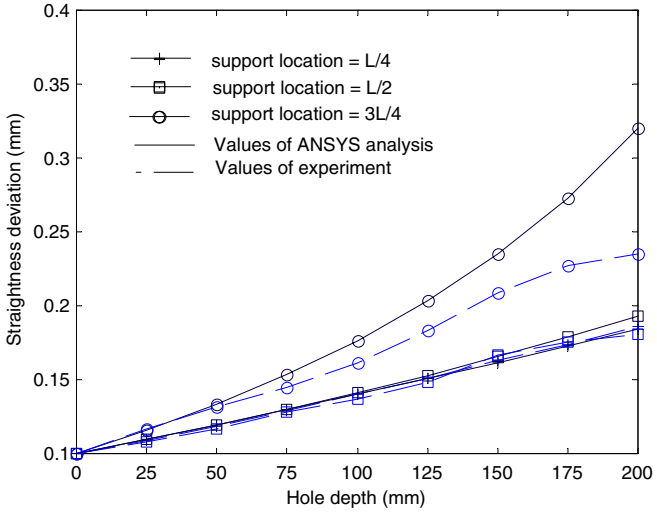

Fig. 20 Hole straightness deviation. Pilot bush misalignment=0.1 mm; tool length=1,600 mm; intermediate support misalignment=0.1 mm

and support misalignment exist. In Figs. 9 and 10 the Sakuma et al.'s model issued the biggest straightness deviation for support distance $l = L/4$ while other models gave similar results. The deviations converged with increasing shaft length (Figs. 10 and 11). Things become different if support distance $l = L/2$, in which case the ANSYS model gave the biggest deviations (Figs. 12 and 13), but again the deviations converged for longer tool shaft (Figs. 13 and 14). With $l = 3L/4$, the ANSYS model gave the diverging straightness deviations while all other mechanisms remain reasonable (Fig. 15). The diverging trend becomes damped for longer tool shaft (Figs. 16 and 17). A dual comparison between ANSYS model and experiment is shown in Figs. 18, 19, 20. It is seen that the support location $l = 3L/4$ always gave the worst straightness deviation, even if the trend is somewhat damped by longer tool shaft.

It is seen from Figs. 21 and 22 that variable support produces smaller straightness deviation than fixed support. Variable support L_{ps}=$L/2$ or an initial fixed support at L_{ps}=$L/2$ results in better straightness while any unbalanced support location, l=$3L/4$ or L_{ps}=$L/4$, produce greater straightness deviation.

The location of support has not been studied in the past, but the FEM model allows an analysis of its influence on the straightness.

5 Conclusions

Deep hole drilling was studied mainly experimentally in the past. Recently, a beam equation was proposed to describe the lateral behavior of the tool shaft, while a

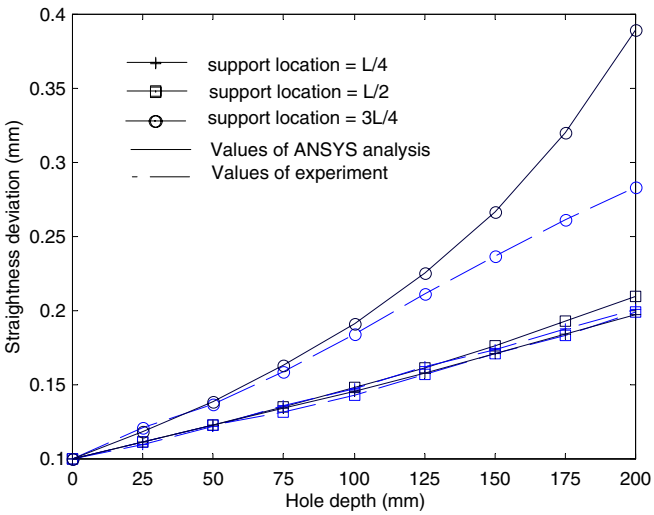

Fig. 19 Hole straightness deviation. Pilot bush misalignment=0.1 mm; tool length=1,400 mm; intermediate support misalignment=0.1 mm

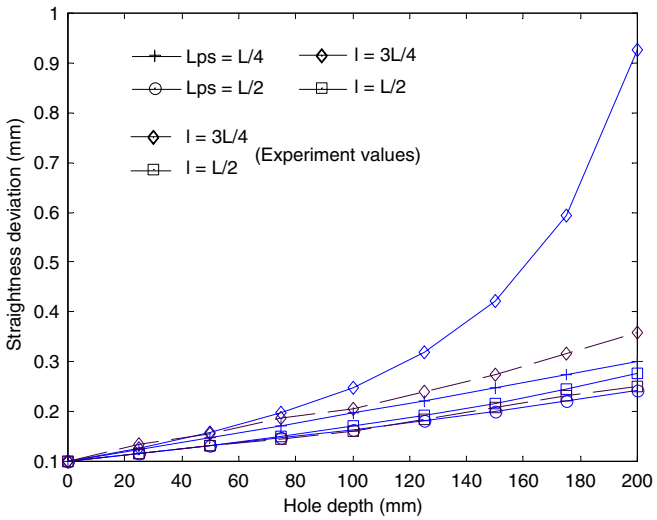

Fig. 21 Influence of various BTA drilling shaft lengths on axial hole straightness deviation. Tool length L=1,000 mm

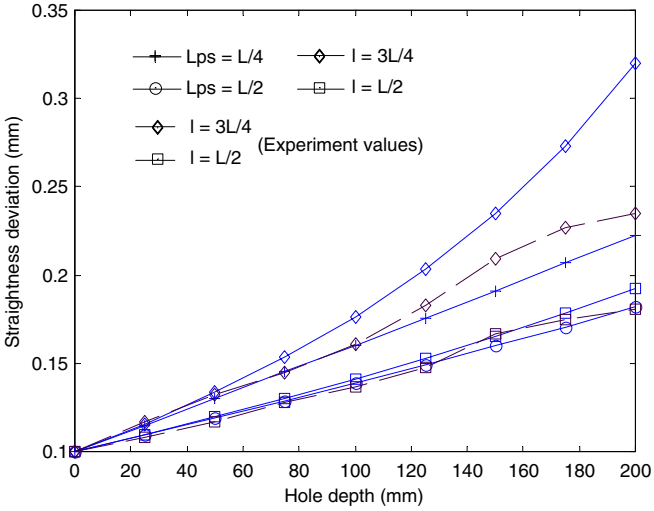

Fig. 22 Influence of various BTA drilling shaft lengths on axial hole straightness deviation. Tool length L=1,600 mm

column equation was needed to describe the straightness deviation caused by bushing and support misalignment. This work constructed a finite element model using PIPE16 elements in ANSYS to investigate deep hole drilling phenomena and compared the strengths and weaknesses of the finite element model with respect to the beam and the column equations.

A first investigation using modal analysis showed that the natural frequencies obtained from the ANSYS model matched those from Chin and Lee's equation [9] and the Euler beam equation. The differences from experimental values are minimal. Static analysis on the ANSYS model showed a prediction ability roughly comparable to the Sakuma et al.'s equation in predicting the straightness deviation in the presence of pilot bushing misalignment; but it was found to be less accurate than that offered by Deng et al.'s column equation [12].

The ANSYS model allowed an analysis of the effect of variable support locations, which neither the beam nor column equation could. The model predicted a smaller straightness deviation for variable support location than for fixed support location.

The investigation in this work showed that the constructed finite element model was a convenient tool in analyzing deep hole drilling which otherwise requires sophisticated beam and column equations; however, it has both strengths and weaknesses. It could predict deviation of the variable support location but was less accurate in predicting the straightness due to pilot bushing misalignment.

References

1. Ramakrishna Rao PK, Shunmugam MS (1987) Accuracy and surface finish in BTA drilling. Int J Prod Res 25(1):31–44
2. Ramakrishna Rao PK, Shunmugam MS (1987) Analysis of axial and transverse profiles of holes obtained BTA machining. Int J Mach Tools Manuf 27(4):505–515
3. Furness RJ, Wu CL, Ulsoy AG (1996) Statistical analysis of the effects of feed, speed and wear on hole quality in drilling. J Manuf Sci E-T ASME 118:367–375
4. Chin JH, Wu JS, Young RS (1993) The computer simulation and experimental analysis of chip monitoring for hole drilling. J Eng Ind 115:184–192
5. Chin JH, Wu JS (1993) Mathematical models and experiment for chip signals of single-edge deep hole drilling. Int J Mach Tools Manuf 33(3):507–519
6. Griffiths BJ (1993) Modelling complex force system, part 1: the cutting and pad forces in deep drilling. J Eng Ind 115:169–176
7. Griffiths BJ, Grieve RJ (1993) Modelling complex force system, part 2: a decomposition of the pad forces in deep drilling. J Eng Ind 115:177–183
8. Chin JH, Lin SA (1996) Dynamic modelling and analysis of deep-hole drilling process. Int J Model Simul 16(3)
9. Chin JH, Lee LW (1995) A study on the tool eigen-properties of a BTA deep hole drill—theory and experiments. Int J Mach Tools Manuf 35(1):29–49
10. Chin JH, Hsieh CT, Lee LW (1996) The shaft behavior of BTA deep hole drilling tool. Int J Mech Sci 38(5):461–482
11. Perng YL, Chin JH (1999) Theoretical and experimental investigations on the spinning BTA deep-hole drill shafts containing fluids and subject to axial forces. Int J Mech Sci 41:1301–1322
12. Deng CS, Huang JC, Chin JH (2001) Effect of support misalignment in deep-hole drill shafts on hole straightness. Int J Mach Tools Manuf 41:1165–1188
13. Kakade NN, Chow JG (1993) Finite element analysis of engine bore distortions during boring operation. J Eng Ind 115:379–384
14. Nelson HD (1996) A finite rotating shaft element using Timoshenko beam theory. J Mech Design 102:793–803
15. ANSYS (1995) User's guide for revision 5.3. Ansys, Inc., Canonburg, PA
16. Sakuma K, Taguchi K, Katsuki A (1981) Self-guiding action of deep-hole-drilling tools. CIRP Ann 30:311–315